Noise-resistant optimal spin squeezing via quantum control

T. Caneva[1], S. Montangero[1], M. D. Lukin[2], and T. Calarco[1]
[1] *Institut für Quanteninformationsverarbeitung, Universität Ulm, D-89069 Ulm, Germany*
[2] *Physics Department, Harvard University, Cambridge, Massachusetts 02138*
(Dated: April 29, 2013)

Entangled atomic states, such as spin squeezed states, represent a promising resource for a new generation of quantum sensors and atomic clocks. We demonstrate that optimal control techniques can be used to substantially enhance the degree of spin squeezing in strongly interacting many-body systems, even in the presence of noise and imperfections. Specifically, we present a time-optimal protocol that yields more than two orders of magnitude improvement with respect to conventional adiabatic preparation. Potential experimental implementations are discussed.

PACS numbers:

Quantum squeezed states are among the most interesting examples of entangled states. In quantum metrology they allow for measurements with an improved precision, ultimately limited only by the Heisenberg limit. Since the early theoretical proposals to realize them with non linear interactions [2, 3], spin squeezed states have been implemented in several experiments. Specific examples include generation of spin squeezed states in cavity QED [4–6], in trapped ions through shared motional modes [7, 8] or using non linear interferometry with a Bose-Einstein condensate [9].

In this Letter we demonstrate that optimal control can be effectively employed to produce highly squeezed spin states in many-body quantum systems, drastically reducing the impact of relaxation and decoherence. We employ the CRAB technique [10, 11] to optimally control the evolution of a collection of N two-level systems mutually coupled through a non linear (i.e. quadratic) interaction. We calculate optimized evolutions occurring on time scales several orders of magnitude shorter than the corresponding adiabatic evolutions, with a speed-up increasing with the system size. Such a speed-up translates directly into an enhanced robustness of the squeezing in the presence of noise, as schematically depicted in Fig. 1. We illustrate this enhanced robustness by modelling two practical experimental implementations of squeezed state preparations: cavity QED and trapped ions [6, 8].

One approach to spin squeezed states is based on the so called one-axis twisting protocol, consisting in letting evolve a collection of two-level systems under the effect of a collective non linear interaction [3], described by a Hamiltonian of the form

$$H_{SM} = \omega J_z + \chi J_x^2 \tag{1}$$

for the global spin variable $\vec{J}$ (see below). Here ω is precession frequency and χ is a strength of nonlinear interaction. The relative simplicity of the one-axis twisting scheme has been at the basis of its ubiquitous presence in squeezing experiments; however such a scheme is known to be non optimal [3], the spherical nature of the angular momentum phase space limiting the maximal squeezing achievable. Such a bound is intrinsic for the one-axis twisting protocol with fixed χ. Sørensen and Mølmer proposed a protocol based on adiabatic evolution to steer a system into maximally squeezed states [12]. This procedure has been implemented experimentally in low-dimensional systems, see for instance Ref. [13]. Unfortunately the required evolution time, which is proportional to the inverse square of the minimum spectral gap Δ encountered during the evolution, $T_{ad} \propto \Delta^{-2}$ [14], scales unfavourably with a system size. This makes adiabatic evolution significantly exposed to external noise: typically in many-body systems the gap closes with increasing system size N, which implies a dramatic increase of the time required for adiabatic evolutions for

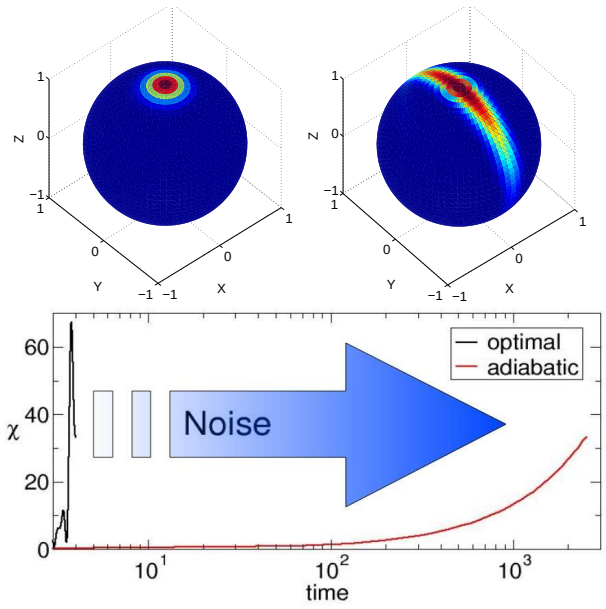

FIG. 1: Upper panel: initial state (left) and final highly squeezed state (right) for a system of $N = 100$ spins. Lower panel: adiabatic (red) and optimal (black) driving fields χ generating the maximally squeezed state shown above; the effect of the noise (big blue arrow) increases with the total evolution time.

large N. Previous studies have demonstrated that optimal control is a powerful tool to drastically reduce the time needed to perform a many-body quantum evolution [11, 15]. In particular the Chopped RAndom Basis (CRAB) technique offers an efficient way to implement optimal control, based on an expansion of the control field onto a truncated basis [10, 11]. Recently it has been shown that optimal control allows for reaching the Quantum Speed Limit (QSL), the minimal time required by physical constraints to perform a given transformation, in spin chains [15, 16], cold atoms in optical lattices [17], Bose-Einstein condensates in atom chip experiments and in crossing of quantum phase transitions [19]. Indeed, CRAB control makes it possible to reduce the time of the transformation down to the QSL, which scales as $1/\Delta$, obtaining a quadratic speedup of the protocol with respect of the adiabatic one. In this work we show that this method is successful also in drastically reducing the preparation time for maximally spin squeezed states, as illustrated in Fig. 1, thereby significantly enhancing the process' robustness to realistic noise sources.

Model — A collection of N two-level atoms having (pseudo)spin $\vec{S}_i$ can be described in terms of the global spin variable $\vec{J} = \sum_{i=1}^{N} \vec{S}_i$, with $|\vec{J}| = N/2$ and z-component J_z representing the population imbalance between the two atomic internal states. In Ramsey spectroscopy experiments, the measured signal M yields the mean global angular momentum pointing along the z-axis, $M \equiv \langle J_z \rangle$, while the noise is given by the uncertainty in one of the orthogonal components $\Delta J_i = \sqrt{\langle J_i^2 \rangle - \langle J_i \rangle^2}$, $i = x, y$. In spin squeezed states, the latter is below the standard quantum limit, i.e. $\Delta {J_i}^2 < |\langle J_j \rangle|/2$ for $i \neq j \in \{x, y, z\}$. The squeezing parameter ξ is defined through the signal to noise ratio as

$$\xi = \frac{\sqrt{2J}\Delta J_x}{|\langle J_z \rangle|}. \tag{2}$$

Squeezed states satisfy the condition $\xi < 1$, which implies entanglement in the system. The ideal states for spectroscopy experiments are those minimizing ΔJ_x for sufficiently large values of the signal, i.e. $M \propto N$. The problem of finding the optimal squeezed state can be recast into the search for the ground state $|\psi_0(\chi, N)\rangle$ of the Hamiltonian Eq. 1, where ω is constant and negative and the non-linear interaction $\chi(t)$ is now taken to be tunable in time [26]. (From now on we set $\hbar = 1$ and time is measured in units of $1/|\omega|$.) Adiabatic evolution under H_{SM} automatically produces optimal squeezed states, as follows: At the time $t = 0$ one takes $\chi(0) = 0$ and the system is prepared in its initial ground state $|\psi_0(0, N)\rangle$, the coherent state $|J_z = J\rangle$ with $\xi = 1$. Then adiabatically increasing $\chi(t)$, the system evolves following the instantaneous ground state $|\psi_0(\chi(t), N)\rangle$ of H_{SM}, yielding exactly the family of states with optimal squeezing at a given value of M (see Fig. 1).

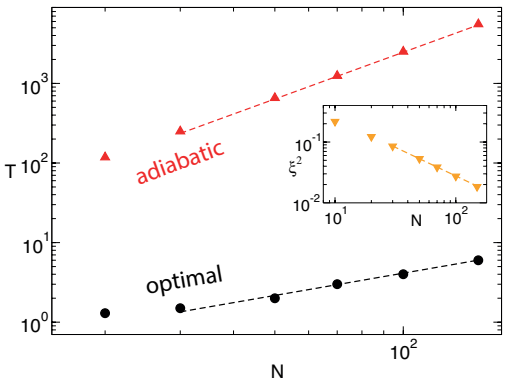

FIG. 2: Scaling with the size of the total evolution time T for the adiabatic ($I_{ad} = 7 \cdot 10^{-3}$, red triangles) and the optimized dynamics ($I_{opt} = 5 \cdot 10^{-4}$, black circles). Numerical fits for $30 \leq N \leq 150$ (dashed lines) result in $T_{ad} \propto N^{1.95}$ and $T_{opt} \propto N^{0.93}$. Inset: Scaling of ξ^2; a fit gives $\xi^2 \sim 2.1/N^{0.94}$.

Optimization in the absence of noise — We first investigate the properties of the Hamiltonian H_{SM} in Eq.(1) to identify target squeezed states that can be reached via adiabatic evolution. We calculate the time required to perform an adiabatic transformation from the initial state into the target and its scaling with the system size N. Subsequently, we apply optimal control to determine the dynamics (neglecting for the moment decoherence effects) leading to the same target state in a much shorter time. Finally, we compare the optimized evolution with the adiabatic one.

As previously mentioned, squeezed states suitable for quantum metrology should have sufficiently strong signal M. To fulfill this requirement we choose (throughout the whole work) $\bar{M} = J/\sqrt{2} = 0.707J$, i.e. $\bar{M} \propto N$. Then we find the value $\chi_{\bar{M}}(N)$ of the interaction such that $|\psi_0(\chi_{\bar{M}}, N)\rangle$ has $\langle J_z \rangle = \bar{M}$ for a given N. The inset of Fig. (2) shows the corresponding value of the ground-state squeezing for varying N: a power-law fit $\xi^2 = A/N^B$ for $30 \leq N \leq 150$ yields $A = 2.1 \pm 0.05$ and $B = 0.94 \pm 0.01$, compatible with the Heisenberg limit $\xi^2 \propto N^{-1}$. This means that we have identified a class of states $|\psi_0(\chi_{\bar{M}}, N)\rangle$ with the desired characteristics. We can now take those states as a target for the optimization, to achieve constant intensity of the signal $\bar{M}$ and maximal squeezing ξ for any given system size N.

As discussed above, the system is initially prepared in the coherent state $|\psi_0(0, N)\rangle$ where all spins are polarized along the positive z-direction and $\xi^2 = 1$, and we aim at reaching the goal state $|\psi_G\rangle \equiv |\psi_0(\chi_{\bar{M}}, N)\rangle$ after an evolution time T. The initial and target state for the case $N = 100$ are depicted in Fig. 1 (upper panels). For the adiabatic case, evolution is computed using a linear ramp $\chi(t) = \chi_{\bar{M}} t/T$. Comparing the resulting final state $|\psi(T)\rangle$ with the goal state yields the infidelity $I = 1 - |\langle \psi_0(\chi_{\bar{M}}, N)|\psi(T)\rangle|^2$. Fig. 2 shows, as a function

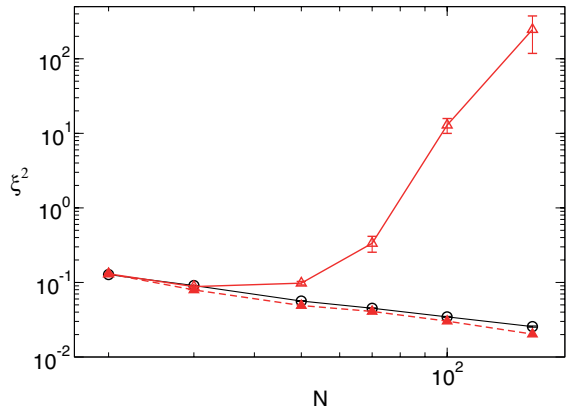

FIG. 3: Final squeezing ξ^2 as a function of the size N, for $\nu = 500$ for the adiabatic (red triangles) and optimal (black circles) dynamics, subject to random telegraph noise with amplitude $K_\alpha = K_\beta = 0.05$ (empty symbols) and $K_\alpha = K_\beta = 0$ (full symbols). Data have been averaged over 24 instances of disorder.

of the size N, the time T_{ad} needed to reach a given infidelity value I_{ad} via adiabatic evolution (red triangles). A fit $T = AN^B$ for $30 \leq N \leq 150$ gives $A = 0.31 \pm 0.01$ and $B = 1.95 \pm 0.01$, in agreement with the prediction of the adiabatic theorem $T_{ad} \sim 1/\Delta^2 \sim 1/N^2$. We then apply the quantum optimal control CRAB algorithm [10, 11] to find the time T_{opt} needed by an optimal transformation to reach an infidelity I_{opt}. More precisely we write the driving field in the form $\chi(t) = \chi_{\bar{M}}[1+\lambda(t)\sum_{j=1}^{n_f} a_j \sin(\omega_j t)+ b_j \cos(\omega_j t)]t/T$, where $\lambda(t)$ ensures constant boundary conditions, $\omega_j = 2\pi/T(1+r_j)$, r_j is a random number, and $n_f \sim O(10)$, and we look for the optimal correction (i.e. the coefficients $\vec{a}, \vec{b}$) such that the infidelity is minimised for a given time (for details on the algorithm and of its complexity see [11, 20]). A typical result is shown in Fig. 1 (lower panel), while the scaling of the optimized evolution time T_{opt} as a function of the size N is shown in Fig. 2 (black circles). A power-law fit $T_{opt} = AN^B$ for $30 \leq N \leq 150$ gives $A = 0.06 \pm 0.01$ and $B = 0.93 \pm 0.04$, consistent with our conjectur about the QSL (see above). This shows that optimal squeezing preparation results in a quadratic improvement in the scaling of the preparation time as a function of the system size, while additionally reducing the total evolution time by at least two orders of magnitude.

Our discussion up to this point neglected completely the effect of noise, which of course is a major concern in a real experiment. Therefore, in order to test the robustness of the protocol, we simulate the dynamics of the system in the presence of noise. We will consider two noise models, as different experimental implementations of squeezed spin states are affected by different kinds of noise. We will show that optimized protocols work also in the presence of these types of noise, and that they are much more resilient to noise than adiabatic protocols.

Effect of classical noise — A typical situation in which classical fluctuations of an external field occur, reflecting in random fluctuations of the interaction strength, is found in trapped ions, also relevant for metrological applications [8]. In trapped ion systems, a global random magnetic noise is expected to be the most relevant source of disturbance [18]. We include it in our simulations by adding random classical telegraph noise to the control field. We then study the evolution induced by the Hamiltonian

$$H = \chi(t)[1 + K_\alpha \alpha(t)]J_x^2 + \omega[1 + K_\beta \beta(t)]J_z \qquad (3)$$

where $\alpha(t), \beta(t)$ are random functions of the time with a flat distribution in $[-1, 1]$, changing random value on average with frequency ν. The case $I_\alpha = I_\beta = 0$ corresponds to a noiseless evolution of Eq.(1). In Fig. 3 we compare the effect of the noise on the final squeezing obtained by varying $\chi(t)$ either linearly in time (empty red triangles) or according to the optimized protocol (empty black circles). The squeezing ξ^2 is plotted as a function of the size N, for $\nu = 500$ and for an intensity of the noise $K_\alpha = K_\beta = 0.05$. As shown in Fig. 3, the noise effect is stronger for larger system sizes, very quickly destroying the squeezing for the slow linear (adiabatic) protocol. The reason is simple: as shown in Fig. 2, for large sizes, e.g. $N \geq 100$, the adiabatic evolution time is three orders of magnitude larger than the optimized one. Vice versa the fast optimal driving turns out to be robust even at large sizes and relatively high intensities of the noise, resulting in a final squeezing almost equivalent to that obtained via the adiabatic process in the absence of noise (full red triangles).

Effect of quantum noise — Finally we discuss a noise model suitable for the description of QED experiments [6], in which the effect of the noise is treated through the formalism of the master equation. In cavity QED, relaxation of the atomic levels towards the ground state and leakage of photons outside the cavity are the most relevant source of dissipation [4]. In order to estimate the effect of the noise in a realistic system, we derive the Hamiltonian of Eq. (1) from a microscopical model. We consider a collection of N three level atoms with two stable ground states $|a\rangle$ and $|b\rangle$ and an excited state $|e\rangle$, in an optical cavity; the ground state energy splitting is given by ω_{ab} and the relevant cavity mode has a frequency ω_0. The stable ground state $|a\rangle$ ($|b\rangle$) is coupled to the excited state with a Rabi frequency Ω_1 (Ω_2) and a frequency ω_1 (ω_2) which is detuned from the excited state by Δ_1 (Δ_2). In the regime of weak laser power, the excited level is almost not populated and it can be adiabatically eliminated, leading to an effective photon-mediated interaction between the two ground state levels $|a\rangle$ and $|b\rangle$. By introducing the total angular momentum operators $J_+ = \sum_{k=1}^N |a\rangle_k\langle b|_k$, $J_- = \sum_{k=1}^N |b\rangle_k\langle a|_k$ and

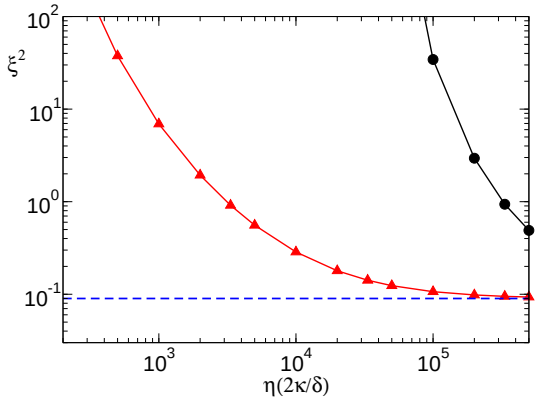

FIG. 4: Squeezing ξ^2 as a function of the cooperativity η in the case of adiabatic (black circles) and optimal (red triangles) protocols with $N = 30$, $2\kappa/\delta \sim 10^{-3}$. The blue dashed line indicates the Heisenberg limit, reached in the large cooperativity limit.

$J_z = (\sum_{k=1}^{N} |a\rangle_k\langle a|_k - |b\rangle_k\langle b|_k)/2$, and by further assuming the strength of the two Raman processes to be identical, $\Omega_1 g_b^*/\Delta_1 = \Omega_2 g_a^*/\Delta_2 = \Omega g^*/\Delta$, after adiabatically eliminating also the cavity field, we obtain the following master equation for the density matrix [27]:

$$\dot{\rho} = -i[\tilde{H}_{eff}, \rho] + \mathcal{L}\rho, \tag{4}$$

with unitary part given by

$$\tilde{H}_{eff} = \chi J_x^2, \tag{5}$$

where $\chi = |\Omega|^2|g|^2/\delta\Delta^2$ and $\delta = \omega_1 - \omega_0 - \omega_{ab}$, and nonunitary part described by the Linbladian

$$\mathcal{L}\rho = \tilde{\gamma}[2J^\dagger\rho J^- - J^-J^\dagger\rho - \rho J^-J^\dagger], \tag{6}$$

where, from a microscopical derivation of the model, the most relevant contribution to the relaxation rate is $\tilde{\gamma} = \chi(t)\gamma\delta/|g^2|$.

Experimental implications — As discussed above, the Hamiltonian Eq. (1) is relevant e.g. for the experiment of Ref. [6]. Here, squeezing of the collective spin of atoms in a cavity is used to improve the measurement precision of an atomic clock. With a realistic estimate of the parameters [6] we have $\Delta = 780$ nm $\sim 3\cdot 10^{14}$ Hz, $\delta \sim 2\pi\cdot 3$ GHz, $\gamma \sim 2\pi\cdot 5$ MHz, $g \sim 2\pi\cdot 0.4$ MHz, $\kappa \sim 2\pi\cdot 1$ MHz. The dominant part for the relaxation is thus proportional to the intensity of driving field χ with a proportionality constant given by $\gamma\delta/|g|^2 \sim 10^5$. Our estimate of relaxation rate can be also expressed in terms of cooperativity $\eta = g^2/(\gamma\kappa)$, leading to $\tilde{\gamma} = \chi(t)\delta/(2\kappa\eta)$, where κ is the decay rate of the cavity. In Fig. 4 the squeezing parameter is shown as a function of η, for a system of size $N = 30$. As clearly shown in the picture, the optimized dynamics requires a cooperativity two orders of magnitude smaller than the one required by the (linear) adiabatic dynamics to reach the same level of squeezing.

Conclusions and outlook — We have shown that optimal control can be used to speed up the dynamics for the production of squeezing, drastically reducing the effect of external dissipation. In particular we have demonstrated that optimized evolutions can occur on time scales orders of magnitude smaller than the corresponding adiabatic evolutions, resulting in maximal squeezed states two orders of magnitude more robust with respect to the noise. The implementation of optimized protocols in spin squeezing experiments could therefore have a great impact in the field of quantum metrology. The very large cooperativity required here to achieve the Heisenberg limit is a consequence of a constraint intrinsic to the scheme of Ref. [4], which aims at a pre-defined state (centered on top of the Bloch sphere as shown in Fig. 1). Relaxing this constraint on the position and orientation of the final state will allow to attain maximum squeezing already with smaller cooperativity. The implementation of closed-loop optimal control strategies might result in additional improvement [25]. Finally application of the present methods demonstrated here to more complex spin squeezing schemes [5], as well as adiabatic quantum computation in the presence of decoherence, can also be envisioned.

We thank NSF, CUA, ARO MURI, Packard Foundation, the SFB TR21 and the European Commission through grants QIBEC and AQUTE for support.

During submission we became aware of the manuscript arXiv:1304.3532 developing an alternative approach to the same problem.

[1] M. Nielsen and I. L. Chuang, *Quantum Computation and Quantum Information*, Cambridge University Press (2000)
[2] D. J. Wineland, J. J. Bollinger, W. M. Itano, and F. L. Moore, Phys. Rev. A **46**, 6797 (1992)
[3] M. Kitagawa and M. Ueda, Phys. Rev. A **47**, 5138 (1993)
[4] A. S. Sørensen and K. Mølmer, Phys. Rev. A **66**, 022314 (2002)
[5] A. André, L. M. Duan, and M. D. Lukin, Phys. Rev. Lett. **88**, 243602 (2002)
[6] I. D. Leroux, M. H. Schleier-Smith, and V. Vuletic, Phys. Rev. Lett. **104**, 073602 (2010)
[7] K. Mølmer and A. S. Sørensen, Phys. Rev. Lett. **82**, 1835 (1999)
[8] D. Leibfried et al, Science **304**, 1476 (2004)
[9] C. Gross, T. Zibold, E. Nicklas, J. Estéve, and M. Oberthaler, Nature **464**, 1165 (2010)
[10] P. Doria, T. Calarco, and S. Montangero, Phys. Rev. Lett. **106**, 190501 (2011);
[11] T. Caneva, T. Calarco, and S. Montangero, Phys. Rev. A **84**, 012312 (2011)
[12] A. S. Sørensen and K. Mølmer, Phys. Rev. Lett. **86**, 4431 (2001)
[13] S. Chaudhury *et al.*, Phys. Rev. Lett. **99**, 163002 (2007)
[14] A. Messiah, *Quantum Mechanics*, North-Holland (1962)

[15] T. Caneva, M. Murphy, T. Calarco, R. Fazio, S. Montangero, V. Giovannetti, and G. E. Santoro, Phys. Rev. Lett. **103**, 1 (2009).
[16] M. Murphy, S. Montangero, V. Giovannetti, and T. Calarco, Phys. Rev. A **82**, 022318 (2010).
[17] M. G. Bason, M. Viteau, N. Malossi, P. Huillery, E. Arimondo, D. Ciampini, R. Fazio, V. Giovannetti, R. Mannella, and O. Morsch, Nature Physics **8**, 147 (2011).
[18] T. Monz et al, Phys. Rev. Lett. **106**, 130506 (2011)
[19] T. Caneva, T. Calarco, R. Fazio, G. E. Santoro, and S. Montangero, Physical Review A **84**, 012312 (2011).
[20] T. Caneva, A. Silva, T. Calarco, R. Fazio, S. Montangero, arXiv:1301.6015
[21] H. J. Lipkin, N. Meshkov, and A. J. Glick, Nucl. Phys. **62**, 188 (1965)
[22] R. Botet and R. Jullien, Phys. Rev. B **28**, 3955 (1983)
[23] J. Larson, EPL **90**, 54001 (2010)
[24] M. H. Schleier-Smith, I. D. Leroux, and V. Vuletic, Phys. Rev. A **81**, 021804(R) (2010)
[25] S. Rosi, A. Bernard, N. Fabbri, L. Fallani, C. Fort, M. Inguscio, T. Calarco, S. Montangero, arXiv:1303.5615.
[26] Indeed the problems are equivalent for J integer; instead for J half-integer the procedure is allowed only if $\langle J_z \rangle / J$ is above a certain threshold, see [12].
[27] see the Supplementary Material for details

Supplementary Material: Microscopical derivation of the model

We consider a collection of N three level atoms with two stable ground states $|a\rangle$ and $|b\rangle$ and an excited state $|e\rangle$ in an optical cavity as done in. [1]. The ground state $|a\rangle$ ($|b\rangle$) is coupled to the excited state with a Rabi frequency Ω_1 (Ω_2) and a frequency ω_1 (ω_2), detuned from the excited state by Δ_1 (Δ_2). The laser frequencies are chosen such that their difference is equal to twice the ground state energy splitting, i.e. $\omega_1 - \omega_2 = 2\omega_{ab}$. With this choice all single atom transitions are off-resonant and atoms can only be excited in pairs. The pairwise excitation of atoms is made possible by the presence of a quantized field inside the cavity coupling both states $|a\rangle$ and $|b\rangle$ to the excited state $|e\rangle$ with coupling constant g_a and g_b, see Fig. 1b for the transition path involving a double Raman process.
Assuming that all fields are propagating in the same direction, the Hamiltonian is:

$$H = \omega_0 c^\dagger c + \omega_{ae}\Sigma_{ee} + \omega_{ab}\Sigma_{bb} + \left[\left(\frac{\Omega_1}{2}e^{-i\omega_1 t} + g_a c\right)\Sigma_{ea} + \left(\frac{\Omega_2}{2}e^{-i\omega_2 t} + g_b c\right)\Sigma_{eb} + h.c.\right], \tag{1}$$

where $\Sigma_{ij} = \sum_{k=1}^{N} |i\rangle_k\langle j|_k$ are collective operators acting on the N atoms.
In order to estimate the effect of the noise, we compute the equation of motion for the ground state coherence $\Sigma_{ab} = J_+$. The corresponding equation of motion takes the following form in a frame rotating at laser frequencies ($H \to \tilde{H}$):

$$i\dot{\Sigma}_{ab} = [\Sigma_{ab}, \tilde{H}] = -\frac{\Omega_1}{2}\Sigma^{(1)}_{eb} + g_b^* c^\dagger e^{-i\delta t}\Sigma^{(1)}_{ae} - g_a c e^{i\delta t}\Sigma^{(2)}_{eb} + \frac{\Omega_2^*}{2}\Sigma^{(2)}_{ae} - i\gamma_0\Sigma_{ab} + (\text{Langevin force}),$$

where γ_0 is the dephasing rate of the ground state coherence, index 1(2) refers to left(right) Raman process in Fig. 1b, and the Langevin force (L.F.) term ensures the commutation relations of the operator. Analogously we can derive the equation of motion for the cavity field:

$$\dot{c} = -i[c, \tilde{H}] = -ig_b^* e^{-i\delta t}\Sigma^{(1)}_{be} - ig_a^* e^{-i\delta t}\Sigma^{(2)}_{ae} - \kappa c + (\text{L.F.}), \tag{2}$$

with κ being the decay rate of the cavity.
In a regime of weak laser power, the excited level is almost not populated and it can be adiabatically eliminated. Therefore in such a regime where $|\Omega|^2/4 \ll \Delta^2 + \gamma^2$, with γ indicating the total decay rate of the excited state $|e\rangle$, we can set $\Sigma_{ee} \sim 0$ and $\dot{\Sigma}^{1(2)}_{ea} = \dot{\Sigma}^{1(2)}_{be} = 0$. With these assumptions the equation of motion for the polarization becomes:

$$\begin{aligned} i\dot{\Sigma}_{ab} \;=\; & -\frac{\Omega_1}{2}\frac{1 - i\gamma/\Delta_1}{\Delta_1}\left[-\frac{\Omega_1^*}{2}\Sigma_{ab} - g_b^* c^\dagger e^{-i\delta t}\Sigma_{bb}\right] + g_b^* c^\dagger e^{-i\delta t}\frac{1 + i\gamma/\Delta_1}{\Delta_1}\left[-\frac{\Omega_1}{2}\Sigma_{aa} - g_b c e^{i\delta t}\Sigma_{ab}\right] \\ & - g_a c e^{i\delta t}\frac{1 - i\gamma/\Delta_2}{\Delta_2}\left[-\frac{\Omega_2^*}{2}\Sigma_{bb} - g_a^* c^\dagger e^{-i\delta t}\Sigma_{ab}\right] + \frac{\Omega_1^*}{2}\frac{1 + i\gamma/\Delta_2}{\Delta_2}\left[-\frac{\Omega_2}{2}\Sigma_{ab} - g_a c e^{i\delta t}\Sigma_{aa}\right] - i\gamma_0\Sigma_{ab} + (\text{L.F.}), \end{aligned}$$

that is, separating the unitary part from the dissipative one

$$\begin{aligned} i\dot{\Sigma}_{ab} = [\Sigma_{ab}, \tilde{H}'] \;=\; & -i\left(\gamma_0 + \frac{\gamma|\Omega_1|^2}{4\Delta_1^2} + \frac{\gamma|\Omega_2|^2}{4\Delta_2^2} + \frac{\gamma|g_b|^2}{\Delta_1^2}c^\dagger c + \frac{\gamma|g_a|^2}{\Delta_2^2}c^\dagger c\right)\Sigma_{ab} \\ & - i\gamma\left(\frac{\Omega_1}{2\Delta_1^2}g_b^* c^\dagger e^{-i\delta t} + \frac{\Omega_2^*}{2\Delta_2^2}g_a c e^{i\delta t}\right)(\Sigma_{bb} + \Sigma_{aa}) + (\text{L.F.}) \end{aligned} \tag{3}$$

where $\tilde{H}'$ is given by

$$\begin{aligned} \tilde{H}' = \; & -\left(\frac{|\Omega_1|^2}{4\Delta_1} + \frac{|g_a|^2}{\Delta_2}c^\dagger c\right)\Sigma_{aa} - \left(\frac{|\Omega_2|^2}{4\Delta_2} + \frac{|g_b|^2}{\Delta_1}c^\dagger c\right)\Sigma_{bb} \\ & - \left(\frac{\Omega_1^*}{2\Delta_1}g_b c e^{i\delta t} + \frac{\Omega_2}{2\Delta_2}g_a^* c^\dagger e^{-i\delta t}\right)\Sigma_{ab} - \left(\frac{\Omega_1}{2\Delta_1}g_b^* c^\dagger e^{-i\delta t} + \frac{\Omega_2^*}{2\Delta_2}g_a c e^{i\delta t}\right)\Sigma_{ba}, \end{aligned} \tag{4}$$

which corresponds to Eq. (A1) of Ref. [1]. The first line of previous equation represents ac-Stark shifts of the ground state: the classical part (proportional to Ω's) can be compensated making a change in the frequency of the fields; the part containing the quantum cavity field is much smaller than the first one and can be neglected in the limit $g^2/\delta\Delta << 1$, see Ref. [1]. Notice that in this limit the part of the dissipation proportional to $c^\dagger c$ can be also neglected.

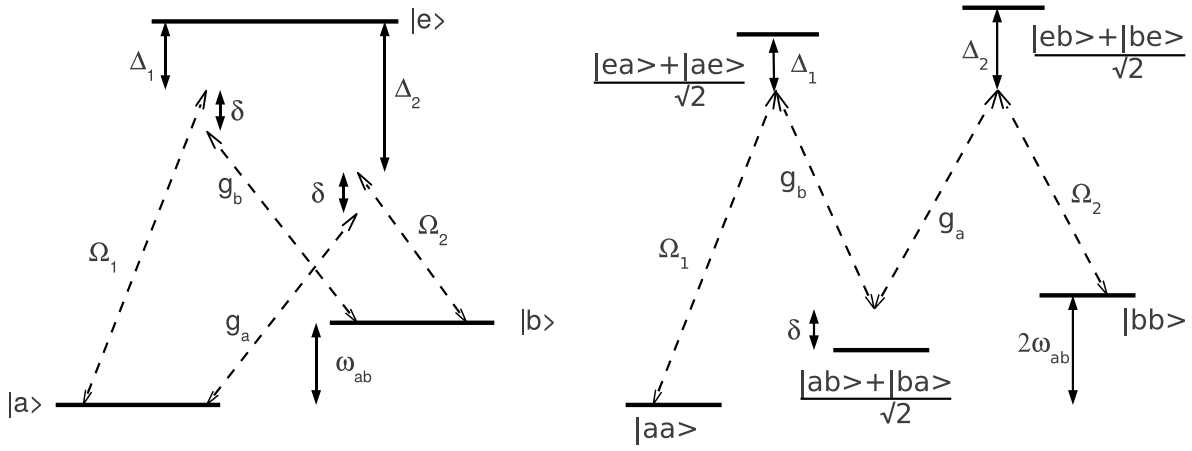

FIG. 1: a) Left panel: Energy levels and couplings. b) Right panel: transition path involving a double Raman process.

In a regime in which the lasers are sufficiently weak and we are not creating a significant number of photon excitations, the cavity field can be also adiabatically eliminated

$$0 = \frac{d(ce^{i\delta t})}{dt} = e^{i\delta t}\frac{dc}{dt} + i\delta c e^{i\delta t},$$

using Eq. (2)

$$ce^{i\delta t} \simeq -\frac{1}{\delta + i\kappa}\left[\frac{g_b^*\Omega_1}{2(\Delta_1 - i\gamma)}\Sigma_{ba} + \frac{g_a^*\Omega_2}{2(\Delta_2 - i\gamma)}\Sigma_{ab}\right] \tag{5}$$

where we are keeping only the 0th-order terms in the cavity field c. Notice that this equation corresponds to Eq. (A3) of Ref. [1]. Therefore inserting Eq. (5) in Eq. (3) and assuming the strength of the two Raman processes to be identical ($\Omega_1 g_b^*/\Delta_1 = \Omega_2 g_a^*/\Delta_2 = \Omega g^*/\Delta$), so that

$$ce^{i\delta t} = -\frac{1 - i\kappa/\delta}{\delta}\frac{\Omega g^*}{2\Delta}\left(\Sigma_{ab} + \Sigma_{ba}\right) \tag{6}$$

we obtain

$$i\dot{\Sigma}_{ab} = [\Sigma_{ab}, \tilde{H}_{eff}] - i\left(\gamma_0 + \frac{\gamma|\Omega|^2}{4\Delta^2} + \frac{\gamma|\Omega|^2}{4\Delta^2}\right)\Sigma_{ab} + i\frac{\gamma}{\Delta}\frac{|\Omega|^2|g|^2}{2\Delta^2\delta}N\left(\Sigma_{ab} + \Sigma_{ba}\right) \tag{7}$$

where we used $\Sigma_{bb} + \Sigma_{aa} \sim N$ and

$$\tilde{H}_{eff} = \frac{|\Omega|^2|g|^2}{4\delta\Delta^2}\left[\Sigma_{ab}\Sigma_{ab} + \Sigma_{ba}\Sigma_{ba} + \Sigma_{ab}\Sigma_{ba} + \Sigma_{ba}\Sigma_{ab}\right]. \tag{8}$$

Finally we can introduce the total angular momentum operators $J_+ = \Sigma_{ab}$, $J_- = \Sigma_{ba}$ and $J_z = (\Sigma_{aa} - \Sigma_{bb})/2$, and the quantity $\chi = |\Omega|^2|g|^2/\delta\Delta^2$ so that previous expressions become:

$$i\dot{J}_+ = [J_+, \tilde{H}_{eff}] - i\left(\gamma_0 + \frac{\gamma\delta}{2|g^2|}\chi\right)J_+ + i\frac{\gamma N}{\Delta}\chi J_x + (\text{L.F.}) \tag{9}$$

with the Langevin force term (L.F.) ensuring validity of the commutation relations for $J_\pm$, and

$$\tilde{H}_{eff} = \chi J_x^2. \tag{10}$$

With a realistic estimate of the parameters [2] we have $\Delta = 780$ nm $\sim 3 \cdot 10^{14}$ Hz, $\delta \sim 2\pi \cdot 3$ GHz, $\gamma \sim 2\pi \cdot 5$ MHz, $g \sim 2\pi \cdot 0.4$ MHz, $\kappa \sim 2\pi \cdot 1$ MHz, so that we obtain for the imaginary part of Eq. (9) $\gamma\delta/|g|^2 \sim 10^5$ and $\gamma N/\Delta \sim 10^{-7}N$. The dominant part for the relaxation is thus proportional to the intensity of driving field χ with

a proportionality constant given by $\gamma\delta/|g|^2 \sim 10^5$, so that we can set in the master equation for the density matrix $\tilde{\gamma} = \chi(t)\gamma\delta/|g|^2$, as discussed in the main article.

[1] A. S. Sørensen and K. Mølmer, Phys. Rev. A **66**, 022314 (2002)
[2] I. D. Leroux, M. H. Schleier-Smith, and V. Vuletic, Phys. Rev. Lett. **104**, 073602 (2010)